

# Monte Carlo Simulation of Vibrational Relaxation in Nitrogen

David P. Olynick\*

*North Carolina State University, Raleigh, North Carolina 27695*

James N. Moss†

*NASA Langley Research Center, Hampton, Virginia 23665*

and

H. A. Hassan‡

*North Carolina State University, Raleigh, North Carolina 27695*

Monte Carlo simulation of nonequilibrium vibrational relaxation of (rotationless)  $N_2$  using transition probabilities from an extended SSH theory is presented. A heating case is examined. For the range of temperatures considered, 4000–8000 K, the vibrational levels were found to be reasonably close to an equilibrium distribution at an average vibrational temperature based on the vibrational energy of the gas. As a result, they do not show any statistically significant evidence of the bottleneck observed in earlier studies of  $N_2$ . Based on this finding, it appears that, for the temperature range considered, dissociation commences after all vibrational levels equilibrate at the translational temperature. These results are a consequence of the fact that the transition probability,  $p(v, v+1)$ , which is a function of energy but not temperature, is an increasing function of the vibrational level  $v$ . Therefore, a behavior similar to that of a harmonic oscillator should be expected.

## Introduction

INTEREST in vibration-dissociation coupling in diatomic gases is a result of its influence on dissociation rates at hypersonic speeds. In this speed range, the time scales of vibrational relaxation and dissociation are closely matched. Thus, vibrational nonequilibrium can slow the rate of dissociation substantially. In spite of the efforts of many earlier investigators,<sup>1–5</sup> which resulted in a number of coupled vibration-dissociation models, the predicted reaction rates were still much faster than the observed rates obtained from experimental data. More recently, Sharma et al.<sup>6</sup> revisited the problem using a generalized SSH (Schwartz et al.) approximation<sup>7</sup> for calculating excitation and dissociation rates of nitrogen. The new approach removed earlier limitations of the theory by using a more accurate representation of the potential in the solution of the Schrödinger equation. Moreover, it incorporated the higher vibrational states and allowed transitions between the bound and the free states. The calculations were carried out for (rotationless) nitrogen, and the probabilities generated by the new calculation were used to calculate the various excitation and dissociation rates assuming a Maxwellian distribution at the translational temperature. Two problems were considered. The first was a heating case where the gas was heated instantaneously from an equilibrium temperature of 4000–8000 K. The evolution of vibrational relaxation was then studied assuming a constant volume and a constant translational temperature. The other involved cooling the gas from 8000 to 6000 K. Based on this study, it was concluded that the (rotationless)  $N_2$  has a bimodal behavior

in which the upper and lower levels reach separate equilibria during relaxation. Moreover, the higher vibrational levels were always in equilibrium with the dissociative states. The results were attributed to the observation that the calculated transition rates had a minimum near the middle of the bound states. This caused a bottleneck in the relaxation from lower to higher vibrational levels, thus slowing the dissociation rate. In general, rates calculated from SSH theory underpredict those obtained from experiment.<sup>8</sup> Because of this, rates used in Ref. 6 were adjusted in such a way so that  $(0 \rightarrow 1)$  rates agreed with experiment.<sup>9</sup>

In a more recent investigation, Sharma and Schwenke<sup>10</sup> studied the vibrational relaxation of  $H_2$  in the presence of rotation. One of their major conclusions was that the bimodal behavior observed for the rotationless  $N_2$  was not observed for  $H_2$  even when it was treated as a rotationless molecule. Moreover, the lower levels tended to overrelax. However, the overrelaxation was not observed when rotationless  $H_2$  was considered.

Both the  $N_2$  and  $H_2$  relaxation studies employed the same master equation approach used in Ref. 6. The major differences between the studies are the treatment of rotational effects and the manner in which the excitation and dissociation rates are calculated. The rates for the  $N_2$  study were calculated using SSH theory, whereas the  $H_2$  study used the quasiclassical trajectory method.<sup>11</sup>

It is not easy to explain the different relaxation behaviors of  $N_2$  and  $H_2$ . One possibility is the inclusion of rotation. The other is the manner in which the vibrational transition and dissociation rates were calculated. Because the resonant V-V transitions dominate all other transitions, one is inclined to discount the role of rotation. This leaves the manner in which the rates were calculated. This issue can be resolved by using the direct simulation Monte Carlo (DSMC) method of Bird<sup>12</sup> because it does not require rates. Implementation of the method only requires reaction cross sections.

The use of the bimodal approximation has far-reaching implications. Based on a study of reentry flows,<sup>13</sup> using the DSMC, it was shown that the assumption results in reduced dissociation and increased convective heating for finite catalytic walls. The increase in convective heating can be as high as 20% for conditions typical of those of the Fire II vehicle. Thus, the first objective of this work is to resolve the bimodal question. The study employs the DSMC method and makes use of the bound-bound and bound-free matrix elements calculated in

Received June 14, 1990; presented as Paper 90-1767 at the AIAA/ASME 5th Joint Thermophysics and Heat Transfer Conference, Seattle, Washington, June 18–20; revision received Sept. 1, 1990; accepted for publication March 19, 1991. Copyright © 1990 by the American Institute of Aeronautics and Astronautics, Inc. No copyright is asserted in the United States under Title 17, U.S. Code. The U.S. Government has a royalty-free license to exercise all rights under the copyright claimed herein for Governmental purposes. All other rights are reserved by the copyright owner.

\*Research Assistant, Mechanical and Aerospace Engineering. Student Member AIAA.

†Research Engineer, Aerothermodynamics Branch, Space Systems Division. Associate Fellow AIAA.

‡Professor, Mechanical and Aerospace Engineering. Associate Fellow AIAA.

Ref. 6 for the calculation of vibrational transition and dissociation cross sections.

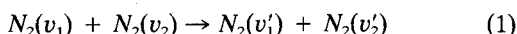
The DSMC method of Bird uses a phenomenological procedure of Larsen and Borgnakke<sup>14</sup> to partition internal energies after a collision. Thus, another objective of this work is to compare the predictions of this phenomenological theory with the evolution obtained using the transition probabilities from the SSH theory.

The results presented here address heating only. As was done in Refs. 6 and 10, the gas is heated instantaneously from an initial equilibrium state and allowed to relax assuming constant volume and translational temperature. Two cases were considered; one involves heating from 4000 to 8000 K and the other from 6000 to 8000 K. The conclusions derived from the two cases were essentially similar. Because of this, only results based on the 4000 to 8000 K case are presented.

### Formulation of the Problem

#### Probability of Vibrational Transitions

The major assumptions of the SSH approximation are that the colliding molecules are rotationless and the collision follows a one-dimensional trajectory in the center of mass frame. The interaction potential of the colliding molecules is approximated by  $V = V_0 \exp(-\alpha r)$ , where  $r$  is the separation distance between the atoms, and  $V_0$  and  $\alpha$  are constants peculiar to the molecular species being considered. Based on this interaction potential, a microscopic transition probability for the reaction



can be obtained from quantum mechanics, where  $v_i$  and  $v'_i$  refer to the initial and the final vibrational states of the nitrogen molecule. This probability is given by<sup>7</sup>

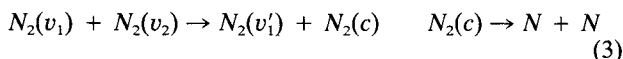
$$P_{v_2 \rightarrow v'_2}^{v_1 \rightarrow v'_1}(u_o) = \frac{1}{16\pi^2} \nu^2(v_1 \rightarrow v'_1) \nu^2(v_2 \rightarrow v'_2) \times (\Theta_o^2 - \Theta_f^2)^2 \frac{\sinh(\Theta_o) \sinh(\Theta_f)}{(\cosh(\Theta_o) - \cosh(\Theta_f))^2} \quad (2)$$

In the above expression,

$$\Theta_o = \frac{4\pi^2 \mu u_o}{\alpha h} \quad \Theta_f = \frac{4\pi^2 \mu u_f}{\alpha h} \quad \frac{\mu}{2} (u_o^2 - u_f^2) = \Delta E = E(v'_1) + E(v'_2) - E(v_1) - E(v_2)$$

where  $\mu$  is the reduced mass,  $\Delta E$  is the total energy exchanged between vibration and translation during a collision,  $u_o$  and  $u_f$  are the initial and final velocities of the relative motion, and  $h$  is Planck's constant.

The probability,  $P_{v_2 \rightarrow v'_2}^{v_1 \rightarrow v'_1}$ , is the steric factor needed for the DSMC method when a hard sphere molecular model is employed. The potential employed in Ref. 6 resulted in 57 vibrational levels for nitrogen. Thus, the vibrational relaxation process can be treated as reactions involving the 57 levels of  $N_2$ . The matrix elements of  $\nu(v - v')$  are calculated in Ref. 6 for cases where  $v'$  is discrete or continuous. As a result, one can consider collisions that result in dissociation, i.e.,



where  $c$  designates a continuum, in the same manner as bound-bound vibrational reactions.

The rate coefficient for the reaction given in Eq. (1) is given in Refs. 6 and 7 as

$$P_{v_2 \rightarrow v'_2}^{v_1 \rightarrow v'_1}(T) = 2 \left( \frac{\mu}{2kT} \right)^2 \int_0^\infty u_o^3 P_{v_2 \rightarrow v'_2}^{v_1 \rightarrow v'_1}(u_o) \exp \left( \frac{-\mu u_o^2}{2kT} \right) du_o \quad (4)$$

where  $k$  is the Boltzmann constant and  $T$  is translational temperature. In principle, the transition probability given in Eq. (2) is valid for all transitions. However, rates generated from Eq. (4) using the transition probability from Eq. (2) do not satisfy detailed balance. To overcome this difficulty, Eq. (2) was multiplied by

$$1 - \frac{\Delta E}{E}$$

when  $\Delta E > 0$  ( $E$  is the relative energy of the colliding molecules) and the lower integration limit was adjusted accordingly. No adjustment in Eq. (4) is necessary when  $\Delta E < 0$ .

#### Simulation Procedure

When two molecules collide, a bound-bound or bound-free transition is possible. The matrix elements for bound-bound transitions,  $\nu(v - v')$ , are numbers. When their values become less than  $10^{-10}$ , the transition is assumed forbidden or negligible.<sup>6</sup> On the other hand, the matrix elements for bound-free transitions,  $\nu(v - c)$ , are functions of the energy of the free state "c." Because of this, it is convenient to treat bound-bound and bound-free transitions separately.

The major steps of the simulation are as follows. First two particles are picked at random. If the particles collide, the possibility of dissociation is checked. If dissociation does not occur, then the probability of a vibrational transition can be calculated. Thus, with repeated applications of this procedure, the vibrational relaxation history can be determined. This procedure will now be described in detail.

The probability of a successful collision is determined in the following manner. After two particles are picked at random, their relative speed,  $u_o \equiv c_r$ , is calculated. The probability of a collision is given by

$$\frac{c_r \sigma_i}{(c_r \sigma_i)_{\max}} \quad (5)$$

where  $\sigma_i$  is the total collision cross section and the subscript max indicates the maximum value. If the above value is greater than  $R_f$ , a random fraction between 0 and 1, the collision will take place. If the collision is successful, dissociation (bound-free transitions) is considered.

To determine if dissociation is possible, the relative translational energy,  $\mu u_o^2/2$ , is calculated. For dissociation to take place, the relative translational energy must be greater than the difference between the dissociation energy and the energy of the molecule in the highest vibrational level, i.e.,

$$\frac{\mu u_o^2}{2} > D - E(m), \quad m = \max(v_1, v_2) \quad (6)$$

where  $D$  is the dissociation energy and  $v_1$  and  $v_2$  are the vibrational levels of the two molecules. If dissociation is possible, an energy,  $E(c)$ , above  $D$  and less than  $E_{\max}$ , the maximum energy for which the matrix elements were calculated, is chosen. The difference in energy,  $E(c) - E(m)$ , gives  $\Delta E$ , which determines the final relative velocity,  $u_f$ . Thus, a steric factor can be calculated. If this number is greater than  $R_f$ , the reaction occurs.

If dissociation does not occur for an  $N_2$ - $N_2$  pair, the possibility of a bound-bound transition is checked. To do this, a final vibrational level is chosen at random for each molecule. The difference between the initial and final vibrational energies,  $\Delta E$  determines  $u_f$  and makes it possible to calculate a steric factor. Again, if the steric factor is larger than  $R_f$ , the transition is accepted. Otherwise, the reaction is treated as an elastic collision, and the above process is repeated.

#### Numerical Considerations

To determine the relaxation behavior of the upper vibrational levels, it is necessary to use a large number of com-

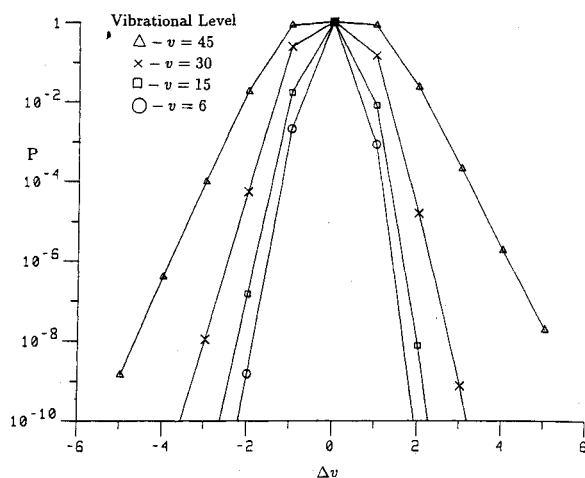


Fig. 1 Calculated vibrational transition probabilities for the reaction  $N_2(v) + M \rightarrow N_2(v \pm v) + M$ .

putational particles, because the population of these states is very small for the present problem. For this study, 400,000 computational particles were used. The memory and computational requirements for this large number of particles require the use of a supercomputer. Calculations in this study were carried out on a Cray Y-MP. To take advantage of the vectorization capabilities of this machine, certain coding strategies had to be adopted. Some of these are now described. The no-time-counter (NTC) method of Bird<sup>15</sup> was used. According to this method, the number of pairs to be sampled in a given time step  $\Delta t_m$  is

$$N_t = \frac{1}{2} N_m n(\sigma_{tr})_{\max} \Delta t_m \quad (7)$$

where  $N_m$  is the number of computational molecules in the cell, and  $n$  is the number density. For a small  $\Delta t_m$ , the number of collision pairs is small relative to the total number of molecules. Therefore, it is good to assume that each particle collides only once during a given  $\Delta t_m$ . This assumption enables the vectorization of the collision process. The collision process is then carried out by picking all possible collision pairs along with an array of random numbers. The collision probabilities are then calculated and compared with the array of random numbers to determine successful collisions. After the conclusion of this process, the velocities of all the particles are reset to maintain a translational temperature of 8000 K and the process is repeated.

The simulation of the bound-bound transition requires the selection of a random vibration level as the final vibrational state for each molecule. This level can be any one of the 57 vibrational levels used in this study. However, for large multilevel jumps, the transition probabilities are near zero. Fig. 1 shows the normalized steric factor for the reaction

$$N_2(v) + M = N_2(v') + M \quad (8)$$

for  $v = 6, 15, 30$ , and  $45$  as a function of  $\Delta v = v' - v$ . For these reactions, the initial relative velocity was chosen to be twice the mean thermal speed. As is seen from the figure for, say,  $v = 6$ , the probability is less than  $10^{-10}$  when  $|\Delta v| > 2$ . This suggests that for  $v = 6$ , successful reactions do not extend beyond two neighbors. On the other hand, when  $v = 45$ , transitions are possible to as many as six neighbors. These observations were confirmed by careful monitoring of successful reactions. Thus, choosing  $v'$  to eliminate the most improbable transitions leads to a significant improvement in the calculation run time.

With the above assumptions, it was possible to obtain an 80% vectorization level in the simulation. This reduced the

run time significantly. However, calculations were still lengthy. This is because of the large number of collisions that must be calculated. As an example, the heating case from 6000 to 8000 K requires the simulation of approximately 8 billion collisions.

Available rate measurements<sup>8</sup> show that SSH theory underpredicts vibrational excitation rates. Unfortunately, no measurements are available for the transition probabilities. Thus, although computed rates were adjusted to match those from experiment in Ref. 6, no adjustments were made in the transition probabilities given by Eq. (2) in this study. Any adjustments would have been empirical in nature and would have been difficult to assess.

## Results and Discussion

In order to compare the results with those of Ref. 6, a heating case in which  $N_2$  is heated instantaneously to 8000 K from an initial equilibrium state of 4000 K is considered. At the initial temperature, the number densities of  $N_2$  and  $N$  are  $1.0 \times 10^{17} \text{ cm}^{-3}$  and  $2.19 \times 10^{14} \text{ cm}^{-3}$ . The gas is allowed to relax assuming a constant volume and a constant translational temperature. The problem is simulated by placing a large number of computational particles in a constant volume. One of the selections that has to be made is the number of computational molecules. Figure 2 shows the expected number of computational molecules in each level at equilibrium assuming a total of  $4 \times 10^5$  computational particles. As is seen from the figure, it is not possible to draw meaningful conclusions about the very high vibrational levels. Initial calculations were performed on a Sun/4 work station using 50,000

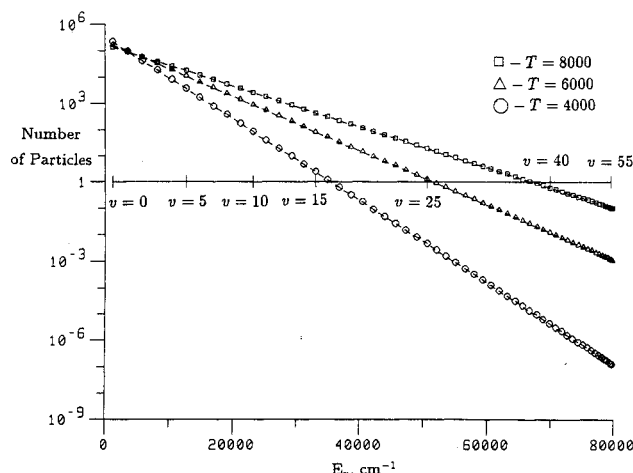


Fig. 2 Expected number of computational molecules in each level for 400,000 particles in equilibrium at various temperatures.

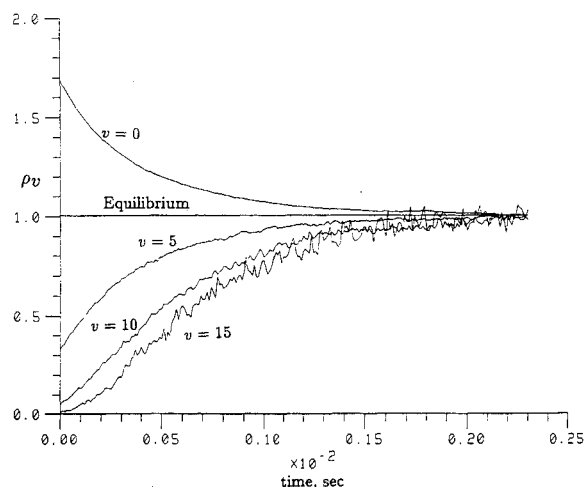


Fig. 3 Time evolution of the normalized vibrational population distribution in a heating environment (4000-8000 K).

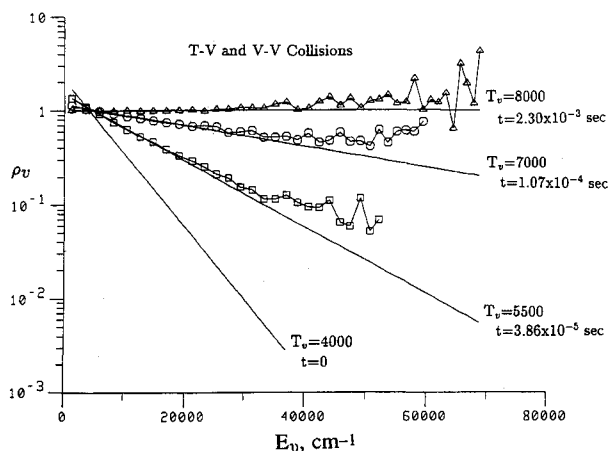


Fig. 4 Comparison of the equilibrium vibrational population distribution at the average vibrational temperature with the actual distribution for various times.

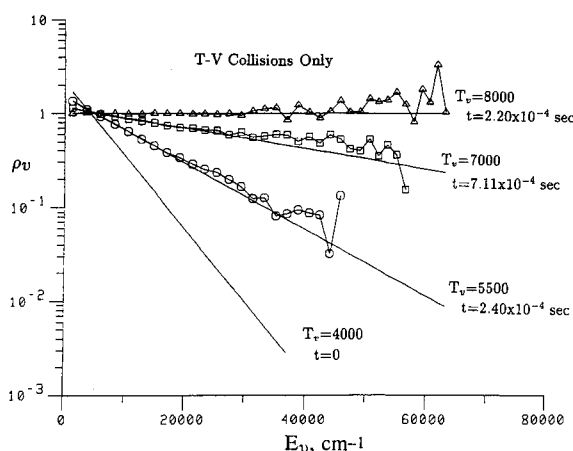


Fig. 5 Comparison of the equilibrium vibrational population distribution at the average vibrational temperature with the actual distribution for various times.

computational molecules. A second calculation was performed on the Cray Y-MP using  $4 \times 10^5$  computational molecules. Both calculations showed identical trends. The code was then vectorized to take advantage of the Y-MP architecture. The speedup due to vectorization was of the order of 40. All results presented here are based on the vectorized version of the code.

Figure 3 shows the manner in which the various levels approach equilibrium. It is a plot of the number of molecules in a given level normalized by the number of particles that will be in that level at equilibrium. Thus, at the beginning of the simulation the number of particles in the ground state is greater than that at equilibrium and  $\rho_v > 1$ . For the upper levels, the numbers at the beginning of the simulation are less than equilibrium values and  $\rho_v < 1$ . As time becomes large,  $\rho_v \rightarrow 1$  for all levels. As is seen from the figure, time requirements to reach equilibrium are almost level independent. Figure 4 shows the evolution of various vibrational levels with time starting from an equilibrium state of 4000 K. Superimposed on the figure are distributions based on the average vibrational temperatures. This temperature was determined from the known vibrational energy and an expression for the equilibrium energy that is determined from the partition function. The partition function is based on the actual vibrational levels and not on a harmonic oscillator assumption. All the levels appear to evolve with an equilibrium distribution based on the average vibrational temperature. The scatter in the upper levels precludes meaningful conclusions about their behavior. Based on the number of successful dissociation re-

actions, it can be safely assumed that vibrational relaxation is complete before dissociation commences. This is consistent with measurements in shock tubes such as those of Camac<sup>16</sup> and Camac and Vaughan.<sup>17</sup> Based on these measurements, the incubation time; i.e., the delay time before dissociation begins, for temperatures below 8000 K is longer than the time necessary to achieve vibrational equilibrium.

When comparing the above results with those of Fig. 3 of Ref. 6, it is noted that the effects of the bottleneck indicated in the figure, which results in the overrelaxation of the intermediate levels and equilibrium amongst the highest levels, is not seen in the present calculation.

Some of the shock tube experiments were carried out using a mixture of diatomic molecules and an (inert) monatomic gas. Such experiments are well represented by the reaction indicated in Eq. (7). Figure 5 shows such a simulation. The transition probabilities for this reaction, which are obtained by setting  $\nu(v_2 - v_2') = 1$  in Eq. (2), are, in general, much higher than those for reaction (1). As a result, equilibrium is reached earlier. However, the trends are identical to those shown in Fig. 4.

Further support for the above results can be seen from Fig. 6. It shows a plot of  $p(v, v+1)$ , which is obtained from Eq. (2) as

$$p(v, v+1) = \sum_{v_2} \sum_{v_2'} P_{v_2 \rightarrow v_2'}^{v \rightarrow v+1}(u_o) \quad (9)$$

The quantity  $\beta^{-1}$  indicated in the figure is the mean thermal speed at 8000 K. The figure shows that  $p(v, v+1)$  increases with  $v$  for a wide range of values of the relative translational energy. The behavior is similar to that of a harmonic oscil-

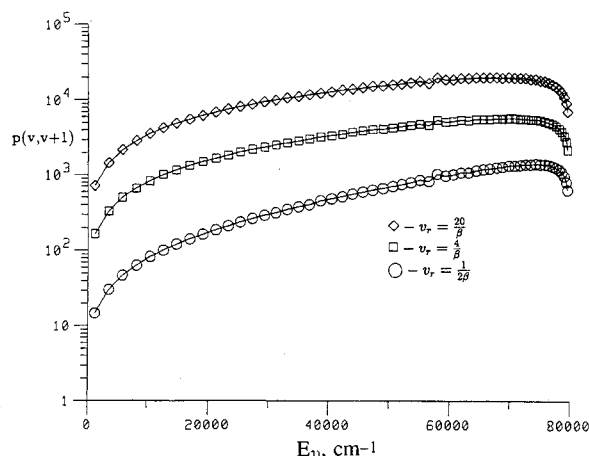


Fig. 6 Next neighbor total transition probabilities for various relative velocities.

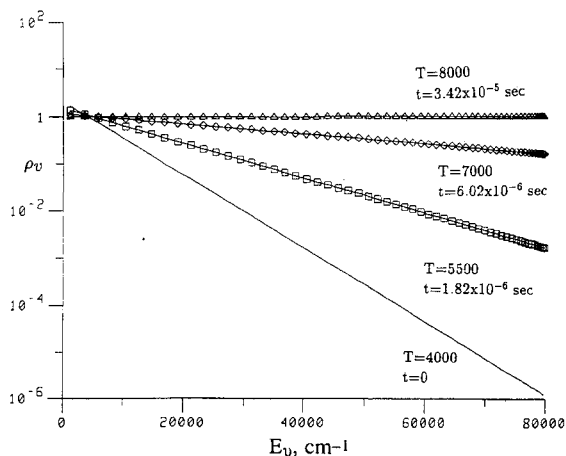


Fig. 7 Average vibrational energy for the Larsen-Borgnakke model.

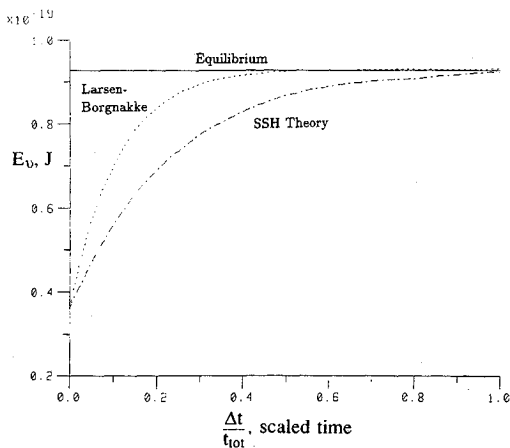


Fig. 8 Comparison of the average vibrational energy as a function of time for SSH theory and the Larsen-Borgnakke model.

lator. Therefore, results typical of harmonic oscillators should be expected.

The DSMC of Bird makes use of the phenomenological method of Larsen-Borgnakke to partition internal energy. As is seen from Fig. 7, calculations based on this procedure result in a distribution consistent with an equilibrium distribution based on the average vibrational temperature. The vibrational relaxation numbers used in Fig. 7, which dictate the time necessary to reach equilibrium, are based on the Millikan and White<sup>8</sup> relaxation times. These times are faster than those resulting from SSH theory. Fig. 8 shows a plot of the evolution of the vibrational energy as a function of the relative time needed to reach equilibrium, where  $t_{\text{tot}}$  is the total time needed to reach equilibrium. As is seen from the figure, the Larsen-Borgnakke procedure represents a good engineering model.

### Concluding Remarks

The present simulation is based on the extended SSH theory. It shows that vibrational relaxation from 4000 to 8000 K of rotationless  $N_2$  proceeds in such a way that all vibrational levels remain in equilibrium at the average vibrational temperature. Based on this simulation, it appears that the major obstacle in developing an accurate theory for coupled vibration dissociation can be traced to the lack of accurate cross sections for dissociation from the various vibrational levels and not to the distribution with which the various levels relax.

### Acknowledgments

This work would not have been possible without the help and support of S. P. Sharma, W. M. Huo, and Chul Park. They provided us with the matrix elements used in the calculation and discussed with us the intricate details involved in the formulation. In addition, the authors thank G. A. Bird

for his guidance and advice. This work is supported in part by NASA's Cooperative Agreement NCCI-112; the Hypersonic Aerodynamic Program Grant NAGW-1022 funded jointly by NASA, AFOSR, and ONR; and the Mars Mission Research Center funded by NASA Grant NAGW-1331. Part of the computer time was provided by the North Carolina Supercomputer Center.

### References

- <sup>1</sup>Hammerling, P., Teare, J. D., and Kivel, B., "Theory of Radiation from Luminous Shock Waves in Nitrogen," *Physics of Fluids*, Vol. 2, 1959, pp. 422-426.
- <sup>2</sup>Treanor, C. E., and Marrone, P. V., "The Effect of Dissociation on the Rate of Vibrational Relaxation," *Physics of Fluids*, Vol. 5, 1962, pp. 1022-1026.
- <sup>3</sup>Marrone, P. V., and Treanor, C. E., "Chemical Relaxation with Preferential Dissociation from Excited Vibrational Levels," *Physics of Fluids*, Vol. 6, 1963, pp. 1215-1221.
- <sup>4</sup>Treanor, C. E., "Vibrational Energy Transfer in High-Energy Collisions," *Journal of Chemical Physics*, Vol. 43, 1965, pp. 532-538.
- <sup>5</sup>Treanor, C. E., Rich, J. W., and Rehm, R. G., "Vibrational Relaxation of Anharmonic Oscillators with Exchange-Dominated Collisions," *Journal of Chemical Physics*, Vol. 48, 1968, pp. 1798-1807.
- <sup>6</sup>Sharma, S. P., Huo, W. M., and Park, C., "The Rate Parameters for Coupled Vibration-Dissociation in a Generalized SSH Approximation," AIAA Paper 88-2714, June 1988, San Antonio, Texas.
- <sup>7</sup>Schwartz, R. N., Slawsky, Z. I., and Herzfeld, K. F., "Calculation of Vibrational Relaxation Times in Gases," *Journal of Chemical Physics*, Vol. 20, 1952, pp. 1591-1599.
- <sup>8</sup>Millikan, R. C., and White, D. R., "Systematics of Vibrational Relaxation," *Journal of Chemical Physics*, Vol. 39, 1963, pp. 3209-3213.
- <sup>9</sup>Park, C., *Nonequilibrium Hypersonic Aerodynamics*, John Wiley, New York, 1989, p. 62.
- <sup>10</sup>Sharma, S. P., and Schwenke, D. W., "The Rate Parameters for Coupled Rotation-Vibration-Dissociation Phenomenon in  $H_2$ ," AIAA Paper 89-1738, June 1989, Buffalo, New York.
- <sup>11</sup>Schwenke, D. W., "Calculation of Rate Constants for the Three-Body Recombination of  $H_2$  in the Presence of  $H_2$ ," *Journal of Chemical Physics*, Vol. 89, No. 4, 1988, pp. 2076-2091.
- <sup>12</sup>Bird, G. A., *Molecular Gas Dynamics*, Oxford University Press, London, 1976.
- <sup>13</sup>Olynick, D. P., Moss, J. N., and Hassan, H. A., "Influence of Afterbodies on AOTV Flows," AIAA Paper 89-0311, Jan. 1989, Reno, Nevada.
- <sup>14</sup>Borgnakke, C., and Larsen, P. S., "Statistical Collision Model for Monte Carlo Simulations of Gas Mixtures," *Journal of Computational Physics*, Vol. 18, 1975, pp. 405-420.
- <sup>15</sup>Bird, G. A., "The Perception of Numerical Methods," *Rarified Gas Dynamics, Progress in Astronautics and Aeronautics*, edited by E. P. Muntz, D. P. Weaver, and D. H. Campbell, Vol. 118, 1989, pp. 211-226, AIAA, Washington, D.C.
- <sup>16</sup>Camac, M., "O<sub>2</sub> Vibrational Relaxation in Oxygen-Argon Mixtures," *Journal of Chemical Physics*, Vol. 37, Feb. 1961, pp. 448-459.
- <sup>17</sup>Camac, M., and Vaughan, A., "O<sub>2</sub> Dissociation Rates in O<sub>2</sub>-Ar Mixtures," *Journal of Chemical Physics*, Vol. 37, Feb. 1961, pp. 460-470.